molecular pharmaceutics

articles

A Novel Rhodamine−Riboflavin Conjugate Probe Exhibits Distinct Fluorescence Resonance Energy Transfer that Enables Riboflavin Trafficking and Subcellular Localization Studies

Mitch A. Phelps,[†] Amy B. Foraker,[‡] Wenqing Gao,[§] James T. Dalton,[†,§] and Peter W. Swaan*[,†,‡]

Biophysics Program and Division of Pharmaceutics, The Ohio State University, Columbus, Ohio 43210-1291, and Department of Pharmaceutical Sciences, University of Maryland, Baltimore, Maryland 21201

Received April 9, 2004

Abstract: Riboflavin (vitamin B_2, RF) is taken up in eukaryotic cells via specialized transport mechanisms. Although RF has fluorescence properties, direct microscopic visualization of RF uptake and trafficking has been complicated by cellular autofluorescence. We describe the synthesis, cellular uptake characteristics, and spectroscopic properties of a novel rhodamine−riboflavin conjugate (RD−RF), including absorption and emission spectra, two-photon excitation spectra, and fluorescence pH dependence. The conjugate has a molar extinction coefficient of 23 670 M^{-1} cm^{-1} at 545 nm (excitation wavelength) with a fluorescence quantum yield of 0.94. This compound exhibits intramolecular fluorescence resonance energy transfer (FRET). Selective quenching of the FRET signal is observed when RD−RF is bound with high affinity by the chicken riboflavin carrier protein. In addition to the typical rhodamine excitation and emission, FRET provides a secondary signal for conjugate localization and an *in situ* mechanism for observing riboflavin binding. Solution and in vitro stability determinations indicate that the linkage between riboflavin and rhodamine is stable for the duration of typical pulse−chase and cellular trafficking experiments. The distinct spectroscopic properties of RD−RF together with a comparable affinity for RF-binding proteins render it an excellent tool for the study of RF transport and trafficking in living cells.

Keywords: Confocal microscopy; fluorescence resonance energy transfer; riboflavin; trafficking; transport; two-photon; vitamin B_2

Introduction

Riboflavin (vitamin B_2, RF) is an essential nutrient that is actively absorbed into eukaryotic cells.[1] Although some prokaryotic transport proteins have been identified, eukaryotic proteins responsible for this mechanism have yet to be discovered. The majority of RF is converted to its cofactor forms, flavin mononucleotide (FMN) and flavin adenine dinucleotide (FAD), and other less prevalent metabolites after RF enters the cell.[2,3] However, only the parent RF form is recognized by the elusive transport system(s). Recent work

* To whom correspondence should be addressed: Department of Pharmaceutical Sciences, University of Maryland, 20 Penn St., HSF2-621, Baltimore, MD 21201. E-mail: pswaan@rx.umaryland.edu. Phone: (410) 706-0103. Fax: (410) 706-5017.

[†] Biophysics Program, The Ohio State University.

[‡] University of Maryland.

[§] Division of Pharmaceutics, The Ohio State University.

(1) Foraker, A. B.; Khantwal, C. M.; Swaan, P. W. Current perspectives on the cellular uptake and trafficking of riboflavin. *Adv. Drug Delivery Rev.* **2003**, *55*, 1467−1483.

(2) Gastaldi, G.; Ferrari, G.; Verri, A.; Casirola, D.; Orsenigo, M. N.; Laforenza, U. Riboflavin phosphorylation is the crucial event in riboflavin transport by isolated rat enterocytes. *J. Nutr.* **2000**, *130*, 2556−2561.

10.1021/mp0499510 CCC: $27.50 © 2004 American Chemical Society
Published on Web 06/08/2004

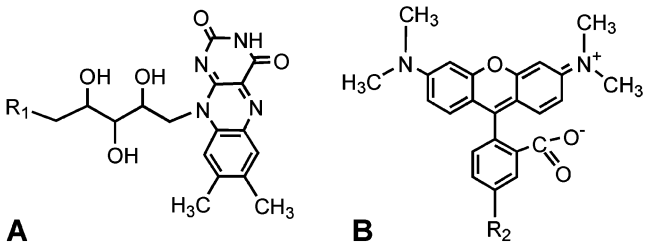

Figure 1. Chemical structures of (A) RF (R_1 = OH; $C_{17}H_{20}N_4O_6$, *m*/*z* 376.14) and (B) RD ($R_2 = NH_2$; $C_{24}H_{23}N_3O_3$, *m*/*z* 401.17). RD−RF is characterized by an R_1R_2 group of OCONH ($C_{42}H_{41}N_7O_{10}$, *m*/*z* 803.29).

by our laboratory shows that receptor-mediated endocytosis (RME) contributes to cellular RF uptake.[4] Our current understanding of RF transport and regulation was recently reviewed.[1]

The isoalloxazine three-ring substructure in RF (Figure 1) behaves like a fluorescent chromophore, but the resulting fluorescence signal is difficult to distinguish from background cellular autofluorescence caused by resident flavoproteins. To overcome this drawback, we synthesized a novel rhodamine−riboflavin conjugate (RD−RF) that allows visualization of cellular trafficking events. RD−RF is a bichromophoric molecule, comprising two fluorescent moieties. Multichromophoric molecules and molecular assemblies are of interest for their potential applications in various areas, including the emerging technologies of molecular electronics and optoelectronics. Electron and energy transfer between chromophores is often observed in such systems, which imparts unique properties not seen in the individual chromophores.[5,6] Our interest in RD−RF stems from its recognition by the natural RF uptake machinery and its RD fluorescence signal. However, further spectroscopic characterization has confirmed that excitation of the donor RF moiety results in fluorescence resonance energy transfer (FRET) to the acceptor RD, which in turn emits a photon in the red region of the spectrum. This is shown through fluorescence spectroscopy and acceptor photobleaching experiments. The FRET signal provides important advantages in using this multichromophoric molecule for transport and trafficking studies. First, the FRET emission provides an additional signal with which to localize the conjugate. Higher sensitivity may be achieved by comparing the RD and FRET signal overlap. Second, the FRET signal may serve as a means of determining if the conjugate is bound by RF-binding proteins. RF carrier proteins (RCPs) are well-characterized in oviparous organisms and appear to be conserved in mammals,[7,8] yet mammalian proteins have yet to be sequenced. Chicken RCP (cRCP) binds tightly to RF and quenches its fluorescence emission. The studies presented herein show that the conjugate RD signal persists while the FRET signal is selectively quenched upon binding to cRCP. Although our studies indicate that the linkage between the RF and RD moieties is stable in cell culture, any hydrolytic or enzymatic cleavage between the RD and RF groups will eliminate the FRET signal, thus providing a potential means of detecting the presence and rate of cleavage of the two fluorophores. Absorbance and fluorescence spectra, including a two-photon (2P) excitation spectrum, were generated, and the fluorescence pH dependence was characterized. Solution and *in vitro* stability studies were performed to ensure that the conjugate is stable for the duration of an experiment. Combined, the data presented herein illustrate the potential of RD−RF for studying RF transport, trafficking, and metabolism. Implications for its use as a model for defining pathways of RF-conjugated drugs are also presented.

Experimental Section

Chemicals. Tetramethylrhodamine-5-carbonyl azide (TMRCA) and 4′,6-diamidino-2-phenylindole (DAPI) were purchased from Molecular Probes (Eugene, OR). The amine derivative of TMRCA (carboxytetramethylrhodamine-4-amine) was purified by preparative HPLC in our laboratory. [^{3}H]Riboflavin (20 Ci/mmol) was purchased from Moravek Biochemicals (Brea, CA). Cell culture media and buffer solutions were from Invitrogen Life Technologies (Carlsbad, CA). RF, flavin mononucleotide (FMN), bovine serum albumin (BSA), and cRCP were purchased from Sigma (St. Louis, MO). BeWo cells were obtained from American Type Culture Collection. Gel/Mount was obtained from Biomeda Corp. (Foster City, CA). All other materials were from Fisher Scientific (Pittsburgh, PA).

Conjugate Synthesis and Purification. Synthesis and purification of RD−RF were modified from our previous methods.[4] RF (5 mg) and TMRCA (0.6 mg; 10:1 molar ratio) were dissolved in dry DMSO (1.0 mL) and heated at 80 °C for 1 h under nitrogen. Reaction samples were mixed 1:3 or 1:6 (v/v) with the mobile phase to a total volume of 250 μL and loaded onto a Beckman C-18 preparative column (5 μm, 10 mm × 25 cm) on an Agilent 1100 series HPLC system and eluted at 3 mL/min with an isocratic mobile phase [34:66 acetonitrile/water mixture containing 0.1% trifluoroacetic acid (TFA)]. An Agilent G1321A fluorescence detector monitored RD emission at 580 nm with dual excitation at 445 and 545 nm. RF was monitored with a G1314A variable-wavelength detector set at 267 nm absorption.

(3) Batey, D. W.; Eckhert, C. D. Identification of FAD, FMN, and riboflavin in the retina by microextraction and high-performance liquid chromatography. *Anal. Biochem.* **1990**, *188*, 164−167.
(4) Huang, S. N.; Phelps, M. A.; Swaan, P. W. Involvement of endocytic organelles in the subcellular trafficking and localization of riboflavin. *J. Pharmacol. Exp. Ther.* **2003**, *306*, 681−687.
(5) Markovitsi, D.; Small, G. Photoprocesses in multichromophoric molecular assemblies: Preface. *Chem. Phys.* **2002**, *2*−*3*, vii−viii.
(6) Wasylewski, Z.; Kaszycki, P.; Guz, A.; Stryjewski, W. Fluorescence-quenching-resolved spectra of fluorophores in mixtures and micellar solutions. *Eur. J. Biochem.* **1988**, *178*, 471−476.
(7) Subramanian, S.; Adiga, P. R. Immunological relatedness of chicken and human riboflavin carrier protein. *Biochem. Biophys. Res. Commun.* **1999**, *262*, 539−544.
(8) Adiga, P. R.; Subramanian, S.; Rao, J.; Kumar, M. Prospects of riboflavin carrier protein (RCP) as an antifertility vaccine in male and female mammals. *Hum. Reprod. Update* **1997**, *3*, 325−334.

Mass Spectrometry. Molecular mass (*m*/*z*) and conjugate purity were verified on a ThermoFinnigan (San Jose, CA) LCQ DECA ion trap mass spectrometer. Positive ion full scan and MS/MS were performed to evaluate purity and confirm the expected chemical structure of each compound.

Absorbance and Fluorescence Spectroscopy. Absorbance spectra of RF, RD, and RD−RF in bathing medium [BM, HBSS with 25 mM glucose and 10 mM HEPES (pH 7.4)] were generated using a 3 mL quartz cuvette on a Hewlett-Packard 8453 UV−vis spectrometer with a fixed 1 nm slit width. Luminescence spectra were recorded on a Perkin-Elmer LS-50B instrument. Varying slit widths (2.5−15.0 nm) were used for single-wavelength excitation and emission measurements. pH dependence studies (4.15−8.41) were carried out in BM. The conjugate fluorescence quantum yield, η, was determined under dilute conditions (2 μM) using the reference method of Demas[9] and the equation

$$\eta_{\text{sample}}/\eta_{\text{reference}} = (\text{Fl}_{\text{area,sample}}/\text{Fl}_{\text{area,reference}})(A_{\text{reference}}/A_{\text{sample}}) \quad (1)$$

where Fl is the integrated area under the corrected fluorescence emission spectrum (in wavenumber scale) for the sample or reference and A is the absorbance of the sample or reference,[10] with RF and RD as standards with quantum yields of 0.25[11] and 0.5, respectively [based on relative measurements of tetramethylrhodamine and Cy5[12] data (Amersham Biosciences)].

Confocal and Two-Photon Imaging. For photobleaching and two-photon (2P) characterization, agarose (100 μg) was added to 200 μL of 2 μM solutions of RF, RD, and the conjugate in BM, and droplets of the mixtures were added to glass slides and sealed under cover slips. Excitation of each suspension was carried out using the Ar and He−Ne lasers of an LSM 510 inverted confocal microscope (Zeiss, Chester, VA) and a tunable Mira 900-F Ti:sapphire laser (Coherent, Hilton, South Australia) equipped with X-wave optics for infrared (IR) output ranges between 700 and 1000 nm. The mode-locked IR laser output power was tuned to a maximum at each 10 nm interval and measured with a FieldMaster GS power analyzer and LM10 QHTD detector head. Single-photon (1P) excitation and photobleaching were performed with the Ar laser 488 nm and the He−Ne laser 543 nm lines through a Zeiss Achroplan IR 40×/0.80 water objective. Light path configurations for both 1P and 2P imaging were established with a high-pass 545 nm dichroic mirror for beam separation through 500−550 nm IR (for RF) and 565−615 nm IR (for RD) filters designed to block stray IR light. Detector gain settings remained constant throughout all acquisitions. For 2P excitation, the mode-locked laser power was tuned to a maximum at each 10 nm wavelength interval, and attenuation was applied via an acousto-optical modulator to minimize the saturation of each image.

Images of the conjugate/agarose mixture in BM were captured at 10 nm intervals. For each image, regions of interest (ROIs) were selected, and average fluorescence intensities were determined. An estimation of the 2P absorption cross section, δ, was determined using the relation[13]

$$\delta \approx \langle F(t)\rangle \frac{2}{\phi \eta_2 C} \frac{f\tau}{g_p} \frac{\pi\lambda}{8n\langle P(t)\rangle^2} \quad (2)$$

where $F(t)$ is the number of photons collected (assuming no quenching or stimulated emission), ϕ is the detector efficiency, η_2 is the 2P quantum efficiency, C is the concentration, g_p is the pulse temporal coherence, f is the pulse rate, τ is the pulse width, n is the refractive index of the aqueous medium, $P(t)$ is the laser power at the focal plane, and λ is the excitation wavelength. Measured pixel intensities were used to estimate the number of photons captured by the photomultiplier tube detectors using the manufacturer's reported quantum efficiency and scaled according to detector gain settings. In addition, 2P cross sections of FMN were calculated and compared to previously published results[13] for further calibration of the $F(t)$ versus pixel intensity relationship. ϕ was determined with 1P excitation of RF, RD, and RD−RF, each with known η_1 values where we assume $\eta_1 = \eta_2$. The value of 0.664 for g_p was assumed for the Ti:sapphire laser pulse with a Gaussian temporal profile.[13] According to the manufacturer's documentation, $f \sim 76$ MHz and $\tau \sim 100$ fs. A value of 1.33 was used for n at all wavelengths, and the use of the IR objective eliminated the need for power attenuation correction in the range of 700−1000 nm.

LSM software was used to calculate average emission intensities within ROIs in the 1024 × 1024 pixel 12-bit two-dimensional image captured at each wavelength. Although control slides of agarose in BM showed no signal with 1P excitation, some signal was observed when using the IR laser. All resulting intensities were therefore corrected with an average ($n = 6$) background subtraction.

For cell imaging, a Nikon Eclipse 800 microscope and camera was used (Nikon Instruments Inc., Melville, NY). A 60×/1.4 oil objective and a 150 μm pinhole were used to capture each image.

Cell Culture. BeWo cells (passage 191−208) were maintained as described previously.[14] For ligand uptake or imaging, BeWo cells were seeded in 24-well plates or 4/8-well culture slides, respectively, and grown to 50−80% confluency. For imaging, cells were pulsed with 300 μL of

(9) Crosby, G. A.; Demas, J. N. The Measurement of Photoluminescence Quantum Yields. *J. Phys. Chem.* **1971**, *75*, 991−1024.

(10) Sun, M.; Moore, T. A.; Song, P. S. Molecular luminescence studies of flavins. I. The excited states of flavins. *J. Am. Chem. Soc.* **1972**, *94*, 1730−1740.

(11) Koziol, J. Studies on flavins in organic solvents. 3. Spectral behaviour of lumiflavin. *Photochem. Photobiol.* **1969**, *9*, 45−53.

(12) Panchuk-Voloshina, N.; Haugland, R. P.; Bishop-Stewart, J.; Bhalgat, M. K.; Millard, P. J.; Mao, F.; Leung, W. Y. Alexa dyes, a series of new fluorescent dyes that yield exceptionally bright, photostable conjugates. *J. Histochem. Cytochem.* **1999**, *47*, 1179−1188.

(13) Xu, C.; Webb, W. W. Measurement of two-photon excitation cross sections of molecular fluorophored with data from 690 to 1050 nm. *J. Opt. Soc. Am. B* **1996**, *13*, 481−491.

ice-cold BM containing 500 nM RF, RD, or RD−RF and fixed as described previously.[4]

Uptake Experiments. Subconfluent BeWo cell monolayers in 24-well plates were washed twice with warm (37 °C) Dulbecco's PBS (pH 7.4) before studies were initiated. RF uptake studies were performed at 37 °C in BM at various concentrations of RF, and the solutions were spiked with [^{3}H]RF. After 20 min, bathing medium was aspirated, and cells were washed twice with ice-cold Dulbecco's PBS (pH 3.0, 2 mL per well for each 2 min wash) to remove free and surface-bound riboflavin.[15] Finally, cells were lysed with a 1% Triton X-100 solution, and the amount of radioactivity in cell lysates was quantitated using a Beckman liquid scintillation counter (model LS 6000IC). The cellular protein content was determined by the BCA method using bovine serum albumin as a standard.

Solution Stability. Aliquots of 2 μM RF, RD, and RD−RF in BM were stored in the dark at −20, 4, and 37 °C. At varying time points, triplicate samples of each compound were pulled from each storage location and incubated in a 37 °C water bath for 5 min; 200 μL was transferred to a white, opaque, flat-bottom 96-well plate and analyzed immediately on a Perkin-Elmer LS-55 luminescence spectrometer. Additionally, 50 μL was blended with 100 μL of acetonitrile (with 0.1% TFA), and 50 μL was injected onto a Nova-Pak C-18 analytical column (3.9 mm × 15 cm). Pumps operated at 1 mL/min with a 5 min gradient from 0 to 30% acetonitrile, and then with a 15 min 30% acetonitrile isocratic flow followed by 5 min re-equilibration at 0% acetonitrile. Calibration curves were constructed (from 0.1 to 10.0 μM) to ensure that the tested concentrations were within the linear range for detection. Peak areas were evaluated at each time point to assess degradation product formation and loss of the parent compound.

***In Vitro* Stability.** BeWo cells were grown in 175 cm^2 culture flasks to 90% confluency. After subsequent washes with PBS and Versene at 37 °C, cells were scraped from the flask and resuspended in BM at a concentration of 1×10^6 cells/mL. A 20 μM solution of RF, RD, or the conjugate was added to the cell suspension, bringing the final concentration to 6×10^5 cells/mL and 8 μM compound. At predetermined time points, aliquots (100 μL) were collected and protein was precipitated with 100 μL of ice-cold acetonitrile containing 0.1% TFA. The suspension was vortexed and then centrifuged at 10000*g* for 2 min, and the supernatant was stored at −80 °C until analysis was carried out.

RF Binding Protein Assays. We used established titration procedures[16,17] to determine binding constants via mutual quenching of RF and cRCP tryptophan fluorescence. The fluorescence intensity of 1.2 μM RF, 0.25 μM RD, and 0.25 μM RD−RF in BM was measured in a 96-well opaque white plate with titration of cRCP or BSA (to assess nonspecific binding). Nonlinear quenching data were fit to an inhibitory Fl_{max} model

$$Fl = Fl_{max} - (Fl_{max} - Fl_0)\frac{C}{C + EC_{50}} \quad (3)$$

where Fl_{max} is the maximum fluorescence (100% in normalized plots), Fl_0 is the minimum fluorescence, and EC_{50} is the protein concentration required to achieve 50% of the total quenching effect. In addition, titration of each compound into 2.0 μM cRCP was conducted to monitor the cRCP tryptophan fluorescence.

Data Analysis and Statistics. Kinetic uptake parameters such as the concentration at half-maximal transport velocity (K_t, Michaelis−Menten-type constant), the maximum uptake velocity (J_{max}), and the passive membrane permeability coefficient (P_m) were calculated using the NONLIN module in SYSTAT (version 8.0, SPSS Inc.) by nonlinear least-squares regression analysis of the obtained data to the general expression

$$J_t = \frac{J_{max}C}{K_t + C} + P_mC \quad (4)$$

where J_t is the total flux and C is the riboflavin concentration. All results are expressed as means ± the standard deviation (SD). Statistical analyses between two groups were performed using a Student's *t* test, and one-way analysis of variance (ANOVA) was used for single and multiple comparisons. Significant differences were reported with a confidence interval of 95%.

Results and Discussion

Conjugate Synthesis and Purification. Reactants and products were separated by preparative HPLC. Two major peaks were identified, collected, and lyophilized. Mass spectrometry analysis of the peak fractions revealed a major singly charged species with ions at *m*/*z* 402.2 [retention time (t_R) of 12.5 min; TMRCA derivative, carboxytetramethylrhodamine-4-amine (RD)] and *m*/*z* 804.3 (t_R = 15.0 min; RD−RF, 60% yield) (Figure 1). The purity of the compounds was confirmed by analytical HPLC to be >95%. A singly charged RD−RF impurity with an ion at *m*/*z* 789.3 was characterized as an ester-linked RD−RF conjugate (Figure 1, R_1R_2 = OCO) as opposed to the carbamate linkage. In addition to RF, HPLC-purified RD was used as a control in most of the studies described herein.

(14) Huang, S. N.; Swaan, P. W. Riboflavin uptake in human trophoblast-derived BeWo cell monolayers: cellular translocation and regulatory mechanisms. *J. Pharmacol. Exp. Ther.* **2001**, *298*, 264−271.

(15) Huang, S. N.; Swaan, P. W. Involvement of a receptor-mediated component in cellular translocation of riboflavin. *J. Pharmacol. Exp. Ther.* **2000**, *294*, 117−125.

(16) Tillotson, J. A.; Bashor, M. M. Fluorometric titration of urinary riboflavin with an apoflavoprotein. *Methods Enzymol.* **1986**, *122*, 234−237.

(17) Choi, J. D.; McCormick, D. B. The interaction of flavins with egg white riboflavin-binding protein. *Arch. Biochem. Biophys.* **1980**, *204*, 41−51.

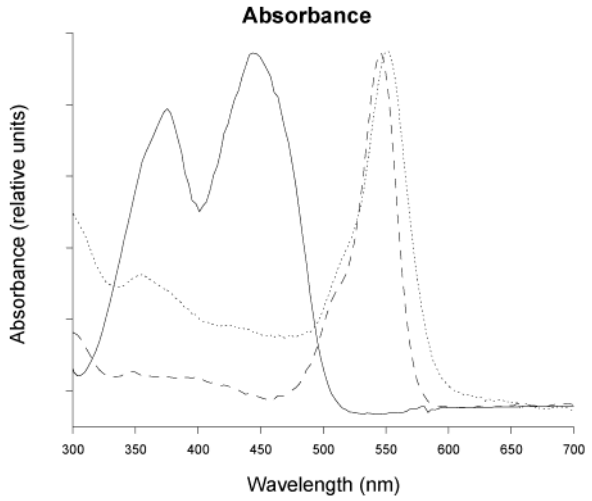

Figure 2. Absorbance spectra of 5 μM solutions of RF (—), RD (- - -), and RD−RF (•••) in BM. Absorbance was measured in a 3 mL quartz cuvette on a Hewlett-Packard 8453 UV−vis spectrometer with a fixed slit width of 1.0 nm. Spectra were normalized for maximum absorption. Extinction coefficients are listed in Table 1.

Table 1. Molar Extinction Coefficients, ϵ, and Fluorescence Quantum Yields, η, for RF, RD, and RD−RF

compound	ϵ_{445} (M^{-1} cm^{-1})	ϵ_{545} (M^{-1} cm^{-1})	η[a]
riboflavin (RF)	11580	–	0.25
carboxy-tetramethylrhodamine-4-amine (RD)	–	82820	0.5
rhodamine-riboflavin (RD−RF)	4070	23670[b]	0.94 (0.03)[c]

[a] Quantum yield values for RF and RD were obtained from literature reports (see the text) and used as references to calculate the values for RD−RF. [b] The extinction coefficient for RD−RF was determined at its maximum absorption at 550 nm. [c] The value of 0.03 represents the quantum yield from the FRET process.

Absorbance Spectroscopy. The normalized absorbance spectrum of RD−RF resembles that of tetramethylrhodamine (Figure 2). The conjugate has an absorption maximum at 550 nm with an extinction coefficient of 23 670 M^{-1} cm^{-1} (Table 1). This maximum is shifted approximately 5 nm from the RD maximum of 545 nm, and the extinction coefficient is approximately one-fourth of the published value of 90 000 M^{-1} cm^{-1} for TMRCA (Molecular Probes Handbook, 2002) or the measured value of 82 820 M^{-1} cm^{-1} for RD (Table 1). In addition, no peak absorbance was observed at 445 nm, as might be expected from the RF moiety. Instead, a broad nearly level absorbance ranging from ~350 to 500 nm was observed. The extinction coefficient of RD−RF was 4070 M^{-1} cm^{-1} at 445 nm, approximately one-third that of RF (Table 1).

Fluorescence Spectroscopy. The fluorescence properties of RF, RD, and RD−RF were compared. Normalized excitation scans were collected while peak emissions were monitored at 521 (Figure 3A) and 575 nm (Figure 3B). Similarly, normalized emission scans were acquired with excitation at 445 (Figure 3C) and 545 nm (Figure 3D), corresponding to the maximum excitation wavelengths for RF and RD, respectively. Typical curves were observed for RF and RD. When emission was monitored at 521 nm, only minimal excitation occurred at 445 nm for RD−RF (Figure 3A). However, when emission was monitored at 575 nm, RD−RF exhibited an excitation curve similar to that of RD, but with a notable increase in the region of 445 nm (Figure 3B). Similarly, emission scans reveal peaks at both 521 and 575 nm for RD−RF with excitation at 445 nm (Figure 3C) and a single peak at 575 nm with excitation at 545 nm (Figure 3D). A control solution with equimolar concentrations of both RF and RD did not exhibit the dual peaks (data not shown), indicating that the energy absorbed by the RF donor moiety with excitation at 445 nm is transferred only to the conjugated RD acceptor group, which in turn emits a photon. This fluorescence resonance energy transfer (FRET) may provide a second signal with which to localize RD−RF in fluorescence microscopy studies. Further, it may serve as a means of assessing intracellular binding of the RF group or perhaps cleavage between the RF and conjugated group.

With excitation at 545 nm, the conjugate exhibits a quantum yield of 0.94, approximately 1.9 times that of RD. An increase in the quantum yield of an acceptor fluorophore may be observed when two potential FRET pairs are conjugated[18,19] or when side groups are modified.[20] The approximate 75% decrease in absorption of the RD moiety is partially compensated by the near doubling of the quantum yield, which will enable an adequate signal to be obtained at a relatively low visible or IR laser power. When RD−RF is excited at 445 nm, its quantum yield measures only 0.03, significantly lower than the value for either RD or RF. This value is also quite different from that of the conjugate when it is excited at 545 nm. If the RD−RF molecule were behaving as a single fluorophore, the quantum yield would be the same regardless of excitation wavelength. We concluded that FRET occurs, but much of the RF excitation energy was lost in internal conversion or other nontransfer and nonradiative processes under the experimental conditions. The Förster distance, R_0, for RF and RD is not available. We are therefore unable to draw further conclusions about the energy loss from the current data. As is typical in FRET pairs, photobleaching of either the donor or acceptor causes a detectable change in the emission of the partner fluorophore.[21] Our results confirm that a slight increase in donor emission (3%) was observed after acceptor bleaching in ROIs (62 and 91% of the initial fluorescence intensity remaining from the red and FRET signals, respectively; data not shown).

(18) Su, J.; Tian, H.; Chen, K. Novel trichromophoric rhodamine dyes and their fluorescence properties. *Dyes Pigm.* **1996**, *31*, 69−77.
(19) Menzel, R.; Thiel, E. Excited-state properties of trichromophoric dye molecules. *J. Phys. Chem. A* **1998**, *102*, 10916−10920.
(20) Menzel, R.; Thiel, E. Intersystem crossing rate constants of rhodamine dyes: influence of the amino-group substitution. *Chem. Phys. Lett.* **1998**, *291*, 237−243.
(21) Andrews, D. L.; Demidov, A. A. *Resonance Energy Transfer*; Wiley: New York, 1999.

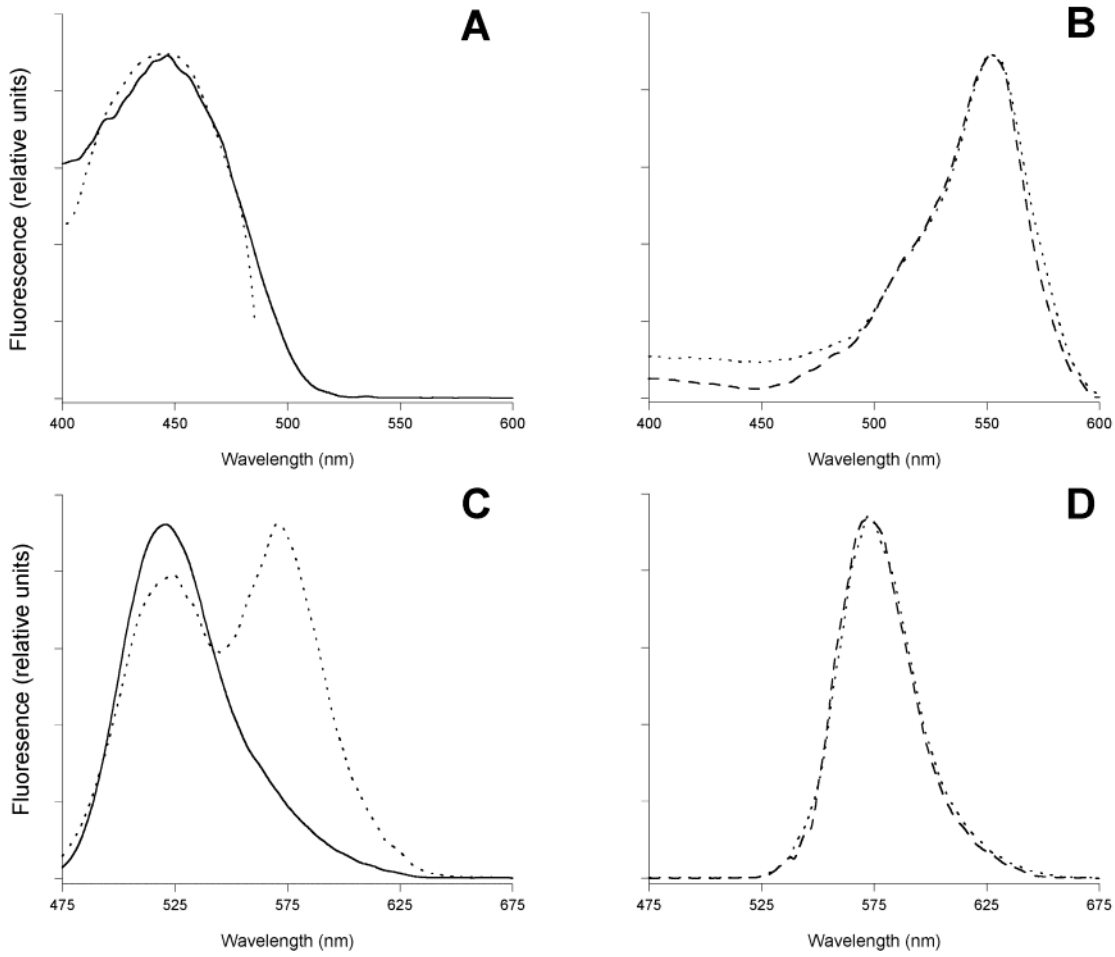

Figure 3. Fluorescence spectra of solutions of RF (—), RD (- - -), and RD−RF (•••) in BM. Fluorescence was measured in a 3 mL cuvette on a Perkin-Elmer LS-50B luminescence spectrometer. Excitation scans monitoring emission at 521 (A) and 575 nm (B). Emission scans with 445 (C) and 545 nm (D) excitation. Slit widths varied between 2.5 and 15.0 nm. The curve for RD−RF in panel A is fitted to the data. All curves were normalized for maximum intensity.

To ensure that RD−RF fluorescence remains constant within the pH ranges to which it may be exposed in the cell, the fluorescence was measured in BM at pH 4.15, 7.42, and 8.51. No significant changes were observed (data not shown).

cRCP Binding Assays. The purpose of RD−RF is to ultimately trace cellular RF absorption and trafficking. Therefore, it is important to verify its specificity for endogenous RF interacting proteins. In addition to our previous data,[4] we assessed the interaction of RD−RF with cRCP. This protein binds RF with a K_d of ~2 nM, resulting in complete quenching of RF fluorescence.[22] Consequently, RD−RF would be expected to bind with high affinity to cRCP. Although quenching of the RF fluorescence in the RD−RF could be monitored, its signal is relatively weak. Alternatively, the FRET signal would provide identical information with higher emission intensity. The RF fluorescence was quenched linearly as a result of high-affinity binding to cRCP (Figure 4A). In contrast, the change in RD fluorescence with an increasing cRCP concentration was insignificant. RD−RF exhibits an intermediate response when monitored with either the FRET (excitation at 445 nm and emission at 575 nm) or red (excitation at 545 nm and emission at 575 nm) channels.

Interestingly, the conjugate FRET signal can be quenched completely ($fl_0 = 0.3\%$), but only approximatey half of the red signal can be quenched ($Fl_0 = 41.6\%$). Given the high affinity of cRCP for RF, the RF moiety of RD−RF is likely bound within the RF binding pocket of cRCP. This is supported by data from experiments recording the cRCP tryptophan fluorescence at increasing RD−RF concentrations (data not shown). If it is assumed that FRET signal quenching is a direct measure of binding of RD−RF to cRCP, $K_d \sim$ 150 nM. Despite an apparent decrease in affinity for cRCP, this value is significantly greater than the values for endogenous RF analogues such as FMN ($K_d = 1.4\ \mu$M) and FAD ($K_d > 14\ \mu$M).[23] The lack of complete quenching for

(22) Nishina, Y.; Horiike, K.; Shiga, K.; Yamano, T. A fluorescence study of egg white riboflavin-binding protein. *J. Biochem.* **1977**, *82*, 1715−1721.

(23) Becvar, J.; Palmer, G. The binding of flavin derivatives to the riboflavin-binding protein of egg white. A kinetic and thermodynamic study. *J. Biol. Chem.* **1982**, *257*, 5607−5617.

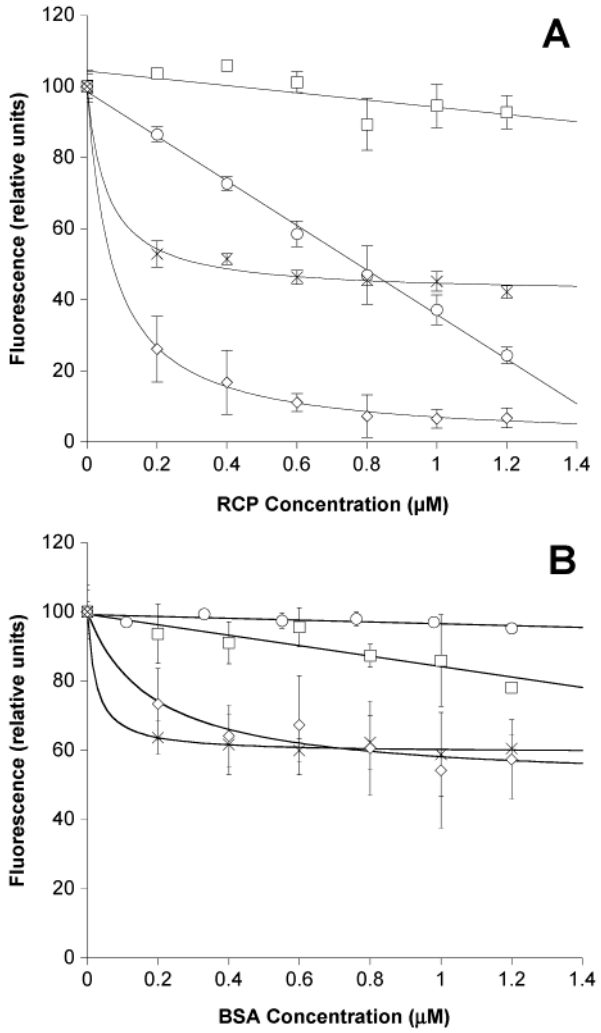

Figure 4. Fluorescence quenching of RF, RD, and RD−RF upon binding to cRCP. Increasing concentrations of cRCP (A) or BSA (B) were added to a 1.2 μM solution of RF (○) and 0.25 μM solutions of RD (□) and RD−RF at 445 (◇) and 545 nm (×) excitation ($n = 3 \pm$ SD). Regression for RF and RD data was linear, whereas RD−RF data were fitted to eq 2. At 445 and 545 nm excitation, the Fl_0 of RD−RF equals 0.3 and 41.6% relative fluorescence units (RFU), respectively, and $EC_{50} = 72$ and 56 nM cRCP. The normalized Fl_{max} equals 100% RFU for both curves.

the red channel suggests that the RD group was not bound by cRCP, consistent with that observed for unconjugated RD. Rather, a change in the quantum yield of the RD group from its conjugated value of 0.94, back to its original value of 0.5, was likely a major cause of the decreased fluorescence signal. Importantly, this residual signal will allow the conjugate to be observed, even when its RF group is quenched by endogenous RF-binding proteins. The RD signal therefore enables localization of RD−RF, and the FRET signal aids in confirmation of conjugate−protein binding.

To determine whether our conjugate can be used to distinguish between specific and nonspecific protein binding, we obtained fluorescence quenching data in the presence of bovine serum albumin (BSA). BSA binds to both RF[24] and RD,[25,26] albeit with affinities and specificities lower than those of cRCP. An apparently saturable quenching was observed with RD−RF in the presence of BSA (Figure 4B). In this case, minimal quenching of the RF signal was observed, while approximately 10% of the RD signal was quenched at the BSA concentrations that were evaluated. Curve shapes for the RD−RF signals were similar to those seen in Figure 4A, but the maximum quenching (minimum fluorescence) in each channel was approximately equivalent with E_0 values of 59.3 and 50.5% for the red and FRET channels, respectively. By comparing the relative signals from the red and FRET channels (red:FRET ratio) for RD−RF, we noticed that specific RF binding results in a large ratio (139 for Figure 4A), while low-affinity RF binding results in a smaller ratio (1.2 for Figure 4B). The RD signal therefore enables localization of RD−RF, and the FRET signal aids in confirmation of conjugate−protein binding with the potential ability to distinguish between RF and RD binding.

Cellular Uptake and Kinetics Studies. We have previously described the presence of a riboflavin transport system in the BeWo cell line.[14] Figure 5 shows the relationship between the uptake of [^{3}H]riboflavin or RD−RF at 20 min and the total RF or RD−RF concentration (1.0−100 nM) in the bathing solution. The rate of control [^{14}C]mannitol uptake ranged from 1.15 to 1.65 pmol/mg of protein at all studied [^{3}H]RF concentrations. After correction for a previously determined nonsaturable transport component,[14] the flux data (J) were fitted to the general expression for Michaelis−Menten-type uptake kinetics; i.e., $J = (J_{max}C)/(K_t + C)$. Nonlinear regression analysis identified an uptake system with an apparent K_t of 1.26 ± 0.21 nM and a J_{max} of 260.3 ± 4.4 fmol (mg of protein)$^{-1}$ (20 min)$^{-1}$ for RF and a K_t of 4.11 ± 0.76 nM and a J_{max} of 14.03 ± 0.34 normalized RFU for RD−RF. These data indicate that RD−RF uptake kinetics are strongly correlated with those obtained using traditional radiolabeled compounds and, thus, can serve as a useful probe molecule for future high-throughput screening assays. Furthermore, RD−RF uptake is significantly inhibited by RF, but not by RD (Figure 5B), and RF uptake is significantly inhibited by RD−RF, but not by rhodamine. Combined, mutual inhibition of uptake demonstrates affinity of the conjugate for an RF-specific uptake mechanism.

Confocal Microscopy and 2P Characterization. 2P excitation is an increasingly popular tool in fluorescence microscopy due to the reduced level of photodamage, the greater penetration depth, the consequent ability to observe

(24) Sawada, O.; Ishida, T.; Horiike, K. Frontal gel chromatographic analysis of the interaction of a protein with self-associating ligands: aberrant saturation in the binding of flavins to bovine serum albumin. *J. Biochem.* **2001**, *129*, 899−907.

(25) Abreu, M. S.; Estronca, L. M.; Moreno, M. J.; Vaz, W. L. Binding of a fluorescent lipid amphiphile to albumin and its transfer to lipid bilayer membranes. *Biophys. J.* **2003**, *84*, 386−399.

(26) Abugo, O. O.; Nair, R.; Lakowicz, J. R. Fluorescence properties of rhodamine 800 in whole blood and plasma. *Anal. Biochem.* **2000**, *279*, 142−150.

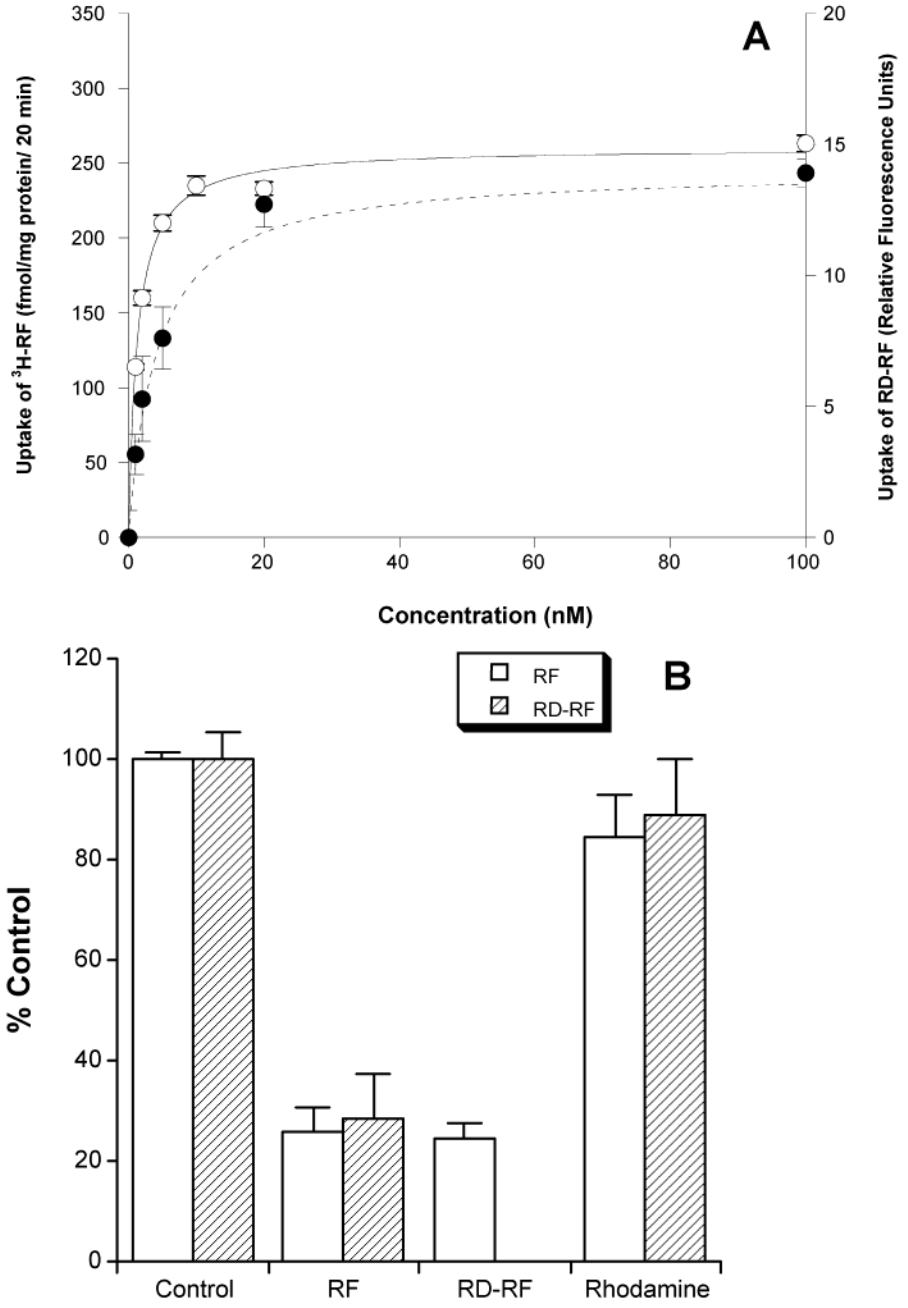

Figure 5. (A) Kinetics of concentration-dependent uptake of [^{3}H]RF and RD−RF in BeWo cells. Cells were seeded in 24-well plates (5×10^4 cells/cm^2) and incubated for 20 min with RF (○) or RD−RF (●) at various concentrations. After subtraction of the passive permeability component, the nonlinear regression lines for RF (—) and RD−RF (- - -) corresponded to K_t values of 1.26 ± 0.21 and 4.11 ± 0.76 nM, respectively, $J_{max} = 260.3$ fmol (mg of protein)$^{-1}$ (20 min)$^{-1}$ and 14.03 ± 0.34 normalized RFU [data are presented as the means ± the standard deviation ($n = 3$)]. (B) Effect of RF, RD−RF, and rhodamine on the uptake of RF and RD−RF. Uptake of [^{3}H]RF (5 nM) and [^{14}C]mannitol (0.39 μM) in BeWo cells were assessed in the absence (control, 100%) or presence of 5 μM RF, RD−RF, or rhodamine (white bars). The uptake of RD−RF was assessed in the absence (control, 100%) or presence of RF or rhodamine (gray bars). After 20 min, cells were washed twice with ice-cold PBS, lysed with 1% Triton X-100, and analyzed for [^{3}H]RF or RD−RF. Each value represents the mean ± SD for three experiments.

living tissue, and the growing availability of pulsed IR lasers. The 2P fluorescence excitation profile of the conjugate was acquired to ascertain the efficacy of RD−RF for monitoring RF absorption and trafficking in real time within living cell and tissue cultures. Figure 6 shows the 2P fluorescence excitation spectra for RD−RF plotted against cross section, δ, in units of GM (10^{-50} cm^4 s photon^{-1}). A broad range of excitation between 700 and 870 nm will produce a sufficient fluorescence signal. Peaks occurred at 710 (222 ± 30 GM), 770 (103 ± 21 GM), and 800 nm (88 ± 26 GM), with a shoulder at ~850 nm (31 ± 25 GM). The results resemble previously reported curves for other RD derivatives (e.g.,

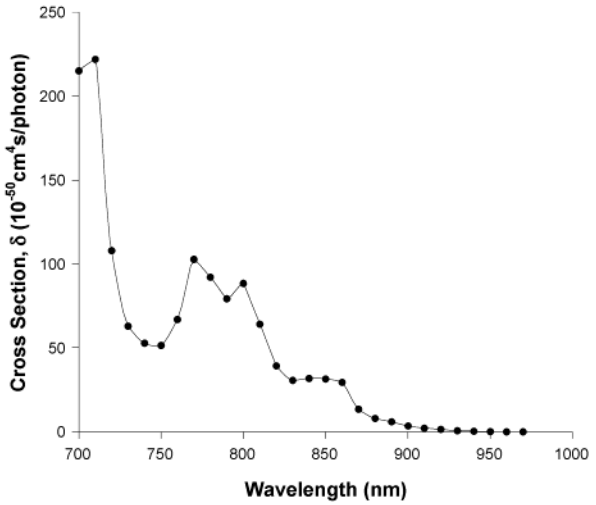

Figure 6. Fluorescence 2P excitation of RD−RF. A 2.0 μM solution of RD−RF was mixed with agarose (as a focal reference) and sealed under glass cover slides (total sample thickness $\sim$ 50 μm). The solution was excited with the Ti:sapphire laser at each 10 nm interval between 700 and 970 nm, and emission intensity was captured as a descanned image by a photomultiplier tube through a 565−615 nm filter designed to exclude IR radiation. Each data point was calculated from image ROI average intensity values (see the text for details of the calculations).

rhodamine B in ref 13), albeit with a slight blue shift for the maxima. We found no reports of studies characterizing 2P absorption or fluorescence excitation of tetramethylrhodamine, although one source mentioned a λ_{max} around 840−850 nm,[27] near the shoulder that we observed for RD−RF. Given that our calculations were based on several assumptions for parameter values, our reported values for δ should be considered approximations. In addition, the 2P fluorescence characteristics of RD−RF may be expected to change depending on the microenvironment within the cell. Nonetheless, this information will be useful in determining acceptable excitation parameters for use of RD−RF in conjunction with other dyes in 2P fluorescence microscopy.

Confocal laser scanning microscopy of subconfluent serum-starved BeWo cells was carried out on microscope culture slides. Cells were pulse-chased with 500 nM conjugate. Fixed cells were stained with 300 nM DAPI nuclear stain. Representative images of the characteristic FRET signal (λ_{ex} = 488 nm, λ_{em} = 580 nm) are shown in red (Figure 7A,D), whereas the DAPI stain is visualized in blue (Figure 7G). Autofluorescence of RF was observed in the FRET (Figure 7A) and green channels (λ_{ex} = 488 nm, λ_{em} = 525 nm) (Figure 7B), but not in the red channel (λ_{ex} = 543 nm, λ_{em} = 590 nm) (Figure 7C). RD−RF-treated cells reveal staining in the FRET (Figure 7D), green (Figure 7E), and red (Figure 7F) channels. Punctate perinuclear staining of the cells reveals distinctly localized uptake into subcellular compartments, presumably endosomes and lysosomes (Figure 7G). Control studies at identical gain levels with untreated cells show only a background signal in the FRET channel (Figure 7A).

Pulse−chase uptake in subconfluent BeWo cells was performed with RD−RF (500 nM) and fluorescein isothiocyanate (FITC) transferrin, a well-characterized marker molecule for clathrin-mediated endocytosis. Distinct regions of punctate endosomal staining around the nuclei (blue DAPI stain) were noted for both the conjugate and transferrin, as observed under the red (excitation at 543 nm and emission at 590 nm) and green (excitation at 488 nm and emission at 525 nm) channels, respectively (Figure 7H). Colocalization of both ligands in identical subcellular compartments was identified and is depicted as yellow regions in Figure 7H. These representative microscopy data re-emphasize the usefulness of RD−RF as a fluorescent probe for RF uptake and trafficking.

Solution and *in Vitro* Stability. Exposure to live cell cultures in aqueous solutions may lead to degradation of RD−RF. Because the FRET signal from the conjugate relies on the linkage between the two fluorophore moieties, its chemical and enzymatic stability during the course of normal fluorescence imaging experiments is an important factor in interpreting the data obtained from such a study. RD−RF is water soluble up to approximately 20 μM. Stability measurements were therefore carried out at 2.0 μM to avoid precipitation during the course of the study. Higher concentrations (8.0 μM) were used for the shorter-term *in vitro* assays. No significant degradation was detected in either study (data not shown). Microplate fluorescence measurements over the 2 week course of solution stability studies at −20, 4, or 37 °C revealed a maximum change of 3% (not statistically significant) for each of the three compounds that were tested (data not shown). HPLC quantitation of the cell-exposed compounds revealed 8% (p = 0.19), 7% (p = 0.19), and 10% (p = 0.13) changes for RF, RD, and RD−RF, respectively. The results suggest that RD−RF is stable in solution, and that its rate of enzymatic degradation is sufficiently slow over the course of a typical 1−2 h incubation used in RD−RF transport and trafficking studies.

Conclusion

The initial purpose of creating RD−RF was to study the transport and intracellular localization of RF. The RD moiety provides a fluorescent signal that is adequately intense and sufficiently separated from regions of the spectrum in which cellular autofluorescence may otherwise interfere with RF detection. We now report additional spectroscopic properties of this conjugate probe with applications in multiphoton excitation and confocal microscopy. Our data indicate that RD−RF exhibits FRET when excited at 488 nm, resulting in emission in the red region of the spectrum. Studies of binding of RD−RF with cRCP demonstrate that the RD signal provides localization, while an attenuated FRET signal may indicate partial quenching due to RF binding. Further,

(27) Schwille, P.; Haupts, U.; Maiti, S.; Webb, W. W. Molecular dynamics in living cells observed by fluorescence correlation spectroscopy with one- and two-photon excitation. *Biophys. J.* **1999**, *77*, 2251−2265.

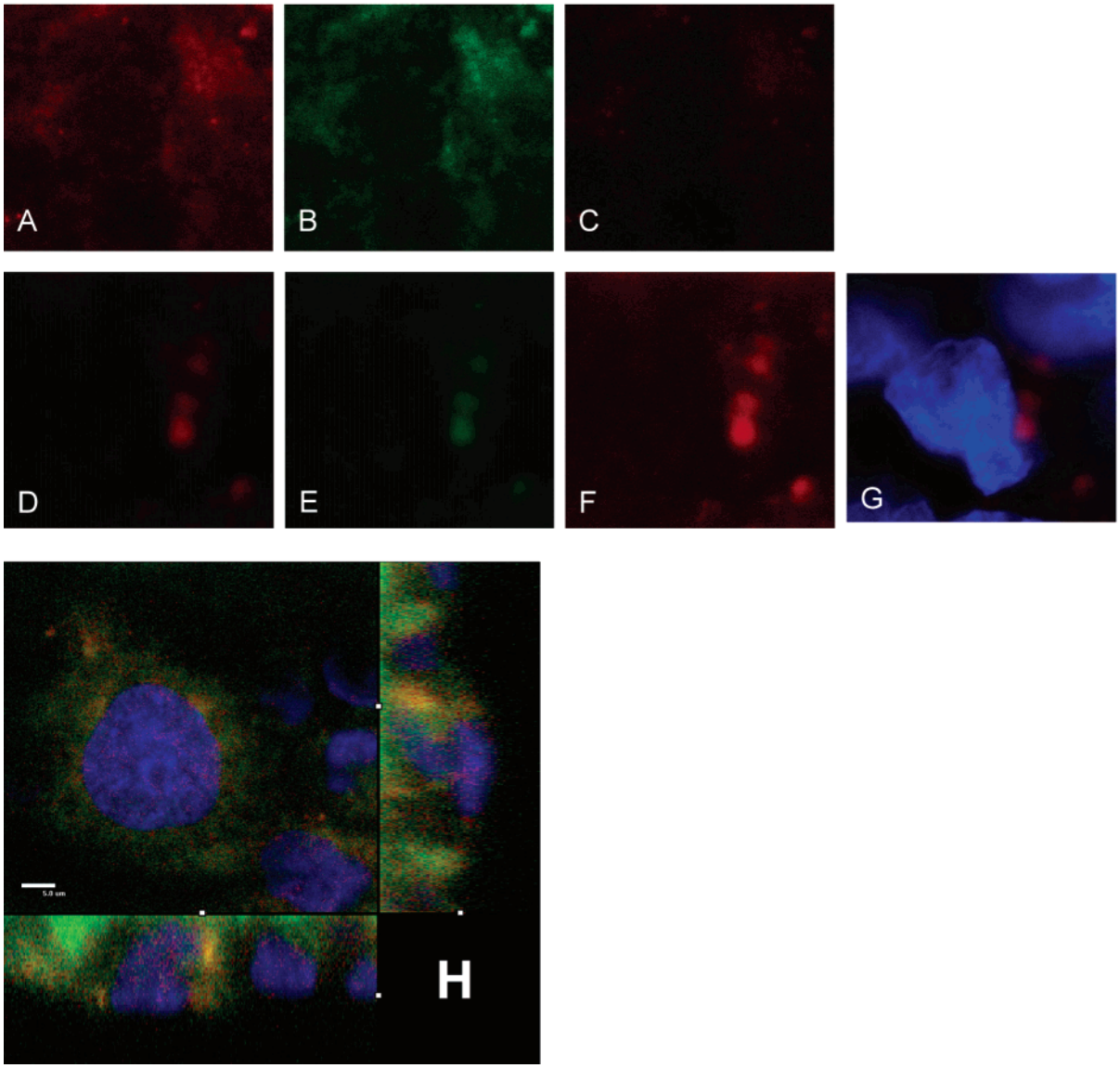

Figure 7. Conjugate signal vs autofluoresence of riboflavin. BeWo cells were serum and nutrient starved for 2 h and then pulsed with either 0.5 μM riboflavin (A−C) or conjugate (D−G) for 2 h at 4 °C, followed by an incubation at 37 °C for 15 min and cell fixation with paraformaldehyde. Internalized substrates were analyzed using confocal laser scanning microscopy. Autofluorescence of riboflavin was seen using the FRET (A) and green (B) channels, but not under the red (C) channel settings. Cells treated with conjugate alone exhibit distinct punctate staining for the conjugate under FRET (D), green (E), and red (F) channels. Further, conjugate (FRET) staining is localized along the nucleus (G). The orthogonal image (H) was acquired using a 60× oil immersion objective (1.4 NA), a z-stack step size of 0.45 μm, a scan period or dwell time of 8.16 μs, 488 argon laser attenuations using neutral density filter 4, and a pinhole setting of 60 μm. A 1024 × 1024 pixel resolution was used, and each slice of the z-stack represents an average of two scans per channel. The bar is 5.0 μm in length.

it appears that ratios of the red, green, and FRET channel signals may prove to be useful for separation and direct quantitation of RF, RD, and conjugate signals. Furthermore, fluorescence-based assays offer high sensitivity and are amenable to rapid assessment with multiwell plate readers. In summary, the distinct spectroscopic properties of RD−RF together with comparable affinity for RF-binding proteins and the RF uptake system in cell culture render it an excellent tool for the study of RF transport and trafficking in living cells.

Acknowledgment. We thank Zengru Wu and Di Wu for their help in obtaining mass spectroscopy data for the conjugate and Alan Bakaletz and Tom Clanton of the Microscopy Core Lab of the Dorothy M. Davis Heart and Lung Research Institute for their generous assistance with the confocal and multiphoton system. This work was supported by National Institutes of Health Grant NIDDK 56631 (to P.W.S.).

MP0499510